Loughborough University

This item was submitted to Loughborough's Institutional Repository (https://dspace.lboro.ac.uk/) by the author and is made available under the following Creative Commons Licence conditions.

creative commons

COMMONS DEED

Attribution-NonCommercial-NoDerivs 2.5

You are free:

- to copy, distribute, display, and perform the work

Under the following conditions:

Attribution. You must attribute the work in the manner specified by the author or licensor.

Noncommercial. You may not use this work for commercial purposes.

No Derivative Works. You may not alter, transform, or build upon this work.

- For any reuse or distribution, you must make clear to others the license terms of this work.
- Any of these conditions can be waived if you get permission from the copyright holder.

Your fair use and other rights are in no way affected by the above.

This is a human-readable summary of the Legal Code (the full license).

Disclaimer

For the full text of this licence, please go to:
http://creativecommons.org/licenses/by-nc-nd/2.5/

Production of O/W emulsions using SPG membranes, ceramic α–aluminium oxide membranes, microfluidizer and a silicon microchannel plate – a comparative study

Goran T. Vladisavljević[a,b*], Uwe Lambrich[b], Mitsutoshi Nakajima[c], Helmar Schubert[b]

[a]Institute of Food Technology and Biochemistry, Faculty of Agriculture, University of Belgrade, P.O. Box 127, YU-11081 Belgrade-Zemun, Serbia, Serbia and Montenegro

[b]Institute of Food Process Engineering, Faculty of Chemical Engineering, University of Karlsruhe (T.H.), Kaiserstrasse 12, D-76128 Karlsruhe, Germany

[c]National Food Research Institute, Tsukuba, Ibaraki 305-8642, Japan

Abstract

O/W emulsions consisting of rapeseed oil as the dispersed phase and 2 wt. % Tween 80 dissolved in demineralized water as the continuous phase were prepared by using different emulsification methods, such as membrane emulsification with Shirasu porous glass and α-Al_2O_3 membranes, microfluidization and microchannel emulsification. The influence of operating conditions and membrane structure on the emulsification process and the emulsion properties was investigated and compared. Under the same conditions and for the same pore size, the SPG membrane enabled to obtain more uniform droplets (span = 0.26-0.45) than α-Al_2O_3 membrane. However, the span of the droplet size distribution of 0.51-0.59 for the α-Al_2O_3 membrane at the wall shear stress of 8 Pa and the dispersed phase flux up to 9 l m^{-2} h^{-1} was significantly smaller than that reported elsewhere for the same membrane type, which was due to careful membrane cleaning

*Corresponding author: Tel: +381 11 615 315 ext. 327; Fax: +381 11 199 711
e-mail address: gtvladis@afrodita.rcub.bg.ac.yu

by ultrasonication. The calculated maximum proportion of active pores for unhindered droplet growth was higher for the α-Al_2O_3 than for SPG membrane, due to the smaller porosity and smaller mean droplet/pore size ratio for the α-Al_2O_3 membrane. At the same $\Delta p_{tm}/p_{cap}$ ratio, the actual proportion of active pores was also higher for this membrane, due to the smaller thickness of active layer. The microfluidization is a suitable method for producing O/W emulsions with a very small mean droplet sizes of 0.085-0.30 μm, that cannot be attained by membrane or microchannel emulsification. However, the span of the droplet size distribution was in the range between 0.91 and 2.7.

Keywords: Membrane emulsification; Microchannel emulsification; SPG membrane; Oil-in-water emulsions; Microfluidizer

1. Introduction

Mechanical emulsification can be carried out using high-pressure homogenizers, rotor-stator systems, ultrasound homogenizers [1] and novel microporous emulsification systems based on a microporous membrane of different structure [2] or regular-sized silicon microchannels fabricated by semiconductor technology [3]. In a microporous emulsification system, small droplets are directly formed by the permeation of dispersed phase through the uniform micro -pores or -channels into moving continuous phase.

Membrane emulsification (ME) was firstly proposed by Nakashima at al. [4] and was initially investigated exclusively using a Shirasu porous glass (SPG) membrane developed by the same authors [5]. In the meantime, this emulsification technology has been attracting an increasing attention all over the world and as a result, other porous

membranes have been also investigated as emulsifying mediums, such as ceramic α-Al_2O_3 and Zr_2O_3 membranes [6-8], silica membranes [9], perforated stainless steel plates [10], polymeric membranes made of different materials such as polypropylene [11], polytetrafluoroethylene [12], and polycarbonate [13], microengineered silicon nitride microsieves [14], etc. However, there are few investigations [6, 15] with the objective of comparing the characteristics of ME process using porous membranes of different structures.

The aim of this study is to compare the emulsification process and the properties of O/W emulsions prepared using SPG and ceramic α-Al_2O_3 membranes under the same operating conditions and using the same chemical composition of both phases. In addition, the results obtained using microfluidizer® and a silicon microchannel plate were also given. The microfluidizer® (Microfluidics Corp., Newton, MA, USA) is a special kind of high-pressure homogenizer, allowing homogenizing pressures up to 275 MPa to be generated. Due to possibility of obtaining very small emulsion droplets, the use of microfluidization was investigated and proposed in many different fields, such as production of sterile-filterable blood substitutes [16], preparation of radioactive particles for use in medical diagnostic imaging [17], homogenization of milk [18], preparation of paper coating binders [19], etc.

2. Experimental

2.1. Materials

Vegetable (rapeseed) oil (Floreal GmbH) with a viscosity of 58 mPa s and a density of 920 kg m^{-3} was used as the dispersed phase. The continuous phase was 2 % (w/w) Tween 80 (polyoxyethylene (20) sorbitan monooleate with an average molecular weight

of 1310 g/mol, Merck GmbH) dissolved in demineralized water. The vegetable oil was treated before usage with 60 g l^{-1} silica gel (Silica gel 60, Merck) to remove all surface-active ingredients and other components which might cause membrane fouling. This treatment involved the adsorption of impurities on silica particles in a stirring vessel for 24 h, followed by centrifugation at 9000 rpm for 2 × 30 min. The viscosity of the continuous phase at 298 K was 1.42 ± 0.01 mPa s determined using a controlled stress rheometer (Carri-Med, CSL-100). The density of the continuous phase at 298 K was 1005 kg m^{-3} determined using a Prolabo tensiometer-densimeter (T.D. 2000).

2.2. Membranes and membrane modules

The SPG membrane tubes were supplied from SPG Technology Co., Ltd (Miyazaki, Japan). The mean pore size of the membrane was determined by a Shimadzu model 9320 mercury porosimeter and was in the range of 0.4-6.6 μm. The membrane tube (125 mm length × 8.7 mm inner diameter × 0.65 mm wall thickness) was installed inside a laboratory made stainless steel module. The effective length of the membrane tube was 115 mm and the effective membrane area 31.3 cm^2.

The ceramic α-Al_2O_3 membranes (250 mm length × 7 mm inner diameter) were supplied from Membraflow GmbH & Co. KG (Aalen, Germany) with a mean pore size of 1.4 and 0.5 μm. These membranes are composed of thin skin layer (with a thickness of 20-30 μm and porosity of 0.35), supported by a porous substructure with thickness of 2 mm. The effective membrane area was 50.0 cm^2.

2.3. Microchannel (MC) plate

The cross-flow silicon MC plate was consisted of microchannels with 16 μm width, 7 μm depth, and 70 μm length containing a terrace with a width of 50 μm and a length of 60 μm. When the terrace length is not zero, the equivalent microchannel diameter is two times larger than the MC depth [20], therefore 14 μm for the given MC plate. The experimental set-up used in this work for MC emulsification was given elsewhere [20].

2.4. Experimental set-up and procedure used for membrane emulsification

The experimental set-up used for membrane emulsification (ME) is shown in Fig. 1. The continuous phase/emulsion was recirculated inside the membrane using a Netzsch model NL 20 Mohno-pump (Waldkraiburg, Germany). This pump was proved to cause no droplet disruption during operation [6]. The tube-side Reynolds number was 1,700-34,000, corresponding to the shear stress at the membrane wall of σ_w = 0.3-140 Pa. A by-pass line was used to decrease flow rate through the module below 200 l h^{-1}.

The dispersed phase was placed in a pressure vessel and introduced at the outer space of the module by compressed air. The continuous phase volume at the beginning of each experiment was 1500 ml (the continuous phase volume inside the pump and pipelines was 900 ml and in the reservoir 600 ml), while the capacity of the pressure vessel was 850 ml. Therefore, the maximum dispersed phase content in the emulsion at the end of each experiment was 36 vol. %. In the most cases, however, the system was operated until a dispersed phase content of 20 vol. % was reached in the emulsion. The weight of oil phase permeated through the pores was measured by a digital balance on which the pressure vessel rested. The balance was interfaced to a PC computer to continuously collect time and mass data using the LabView® software.

After each experimental series, the whole ME system was cleaned in place with 1 % (w/w) cleaning agent P3-ultrasil 53 (Henkel KGaA) at 323 K. After CIP cleaning, the module was dismantled and the membrane (SPG or α-Al_2O_3) was additionally cleaned in an ultrasonic bath for at least several hours using commercial detergent solutions.

2.5. Experimental set-up and procedure used for microfluidization

The experimental set-up used for microfluidization (MF) is shown in Fig. 2. The pre-emulsion containing 1-50 vol. % of the dispersed phase was prepared in a stirring vessel and was introduced into the homogenizing valve at the operating pressures ranging from 5 to 110 MPa. Inside the valve the premix is divided into two streams which join into a single stream afterwards. In this study, a single pass or two consecutive passes of emulsion through the system were applied. In the latter case, the emulsion prepared in the first homogenization was passed through the valve in the second pass.

2.6. Determination of mean droplet size and droplet size distribution

Droplet size distribution for all samples was measured by a Coulter LS 230 light scattering particle size analyser using PIDS technology, which allowed the detection of droplets in the range of 0.04-2000 μm. The mean droplet diameter was expressed as the mean Sauter diameter, $d_{3,2}$. The droplet uniformity was expressed as the span of droplet size distribution: span = $(d_{90}-d_{10})/d_{50}$, where d_{x0} is the diameter corresponding to x0 vol. % on a relative cumulative droplet size distribution curve. This parameter was termed by some authors [21] as the particle size dispersion coefficient.

3. Results and discussion

3.1. Pure water permeability of the SPG and α-Al_2O_3 membranes

Fig. 3 shows the pure water flux, J_w, through the SPG and α-Al_2O_3 membranes at different transmembrane pressures, Δp_{tm}. As expected, a linear relationship between J_w and Δp_{tm} was obtained and the slope of these lines increased with increasing the mean pore size. In addition to that, the 1.4 μm-α-Al_2O_3 membrane was less permeable to pure water than the SPG membrane with the same pore size. It was due to a thick support layer of the α-Al_2O_3 membrane. The hydraulic membrane resistance, R_m, was calculated from the slope of the J_w vs. Δp_{tm} lines using the equation: $R_m = (\eta_w \partial J_w / \partial \Delta p_{tm})^{-1}$, where η_w is the viscosity of pure water at operating temperature.

As shown in Fig. 4, the hydraulic resistance of the SPG membrane was independent on the effective membrane area. A linear relationship between R_m and d_p was obtained in logarithmic coordinates, with a slope of -2 [22]: $R_m = 0.056 d_p^{-2}$, where R_m and d_p are in m^{-1} and m, respectively. According to our previous study [22], the mean wall porosity of the SPG membranes used here was ε = 0.58. Thus, the mean tortuosity factor of the pores can be calculated from the Hagen-Poiseuille law using the equation:

$$\xi = \sqrt{\frac{R_m \varepsilon}{32 d_p \delta_m}} = \sqrt{\frac{0.056\varepsilon}{32\delta_m}} = \sqrt{\frac{0.056 \times 0.58}{32 \times 0.65 \times 10^{-3}}} = 1.25 \qquad (1)$$

The mean tortuosity of 1.25 is very similar to 1.32 reported by Nakashima and Shimizu [23] for the same type of membrane. The α-Al_2O_3 membrane was less resistive than the SPG membrane at the mean pore size of 0.5 μm, but more resistive at d_p = 1.4 μm. Presumably, the contribution of porous substructure to the overall resistance is less significant at the smaller mean pore size and thus, the α-Al_2O_3 membrane is less resistive due to thin skin layer. At d_p = 1.4 μm, the proportion of supporting layer in

overall resistance is higher and the α-Al_2O_3 membrane is more resistive than the SPG membrane due to both a thick supporting layer and the smaller porosity of active layer.

3.2. Influence of emulsification method on the droplet size distribution

As shown in Fig. 5, the SPG membrane enabled to produce the O/W emulsions with a very narrow droplet size distribution over a wide range of mean pore sizes at a small wall shear stress of 8 Pa. The span of the droplet size distribution of 0.26-0.45 for the SPG emulsification was much lower than 0.94-2.7 for the microfluidization at the homogenizing pressure of 5-110 MPa (Tab. 1). On the other hand, the microfluidizer® is a suitable apparatus for the production of O/W emulsions with the mean droplet sizes of less than 0.3 μm, on the condition that the dispersed phase content is up to 20 vol. % and that the homogenizing pressure is high enough. Furthermore, using two passes of emulsion through the homogenizing valve at 110 MPa, the mean droplet sizes of only 0.085-0.087 μm were obtained at the dispersed phase content of 1-2.5 vol. %. Using the SPG membrane with the smallest available mean pore size of 0.05 μm, a mean droplet size of over 0.17 μm could be expected. However, due to some problems which are still unsolved till now, such as leakage between the O-ring and outer membrane surface, it is not easy to prepare a monodispersed emulsion with the mean droplet size of less than 0.5 μm using SPG membranes [24].

At the same pore size and under the same experimental conditions, the oil droplets produced by utilizing the SPG membrane were more uniform than droplets prepared by using the α-Al_2O_3 membrane. (Fig. 5). However, the obtained span values of 0.51-0.59 for the α-Al_2O_3 membrane at the wall shear stress of 8 Pa and the dispersed phase flux up to 9 l m^{-2} h^{-1} were much smaller than those reported by other authors [6-8] for the

same membrane type. E.g., Williams et al. [7] have obtained the span of 0.83 at the oil flux of 8 l m^{-2} h^{-1} using an α-Al_2O_3 membrane with the mean pore size of 0.5 μm. We believe that a narrower droplet size distribution in our experiments was due to a careful membrane cleaning by ultrasonication. This treatment was essential to completely clean the membrane pores and was not performed by other authors [6-8].

It should be noted here that the span of droplet size distribution for the emulsions prepared by MC emulsification was close to the upper limit for SPG emulsification. The additional experiments are necessary to confirm this statement.

3.3. Influence of operating parameters on the mean droplet size and dispersed phase flux

As shown in Fig. 6, the dispersed phase flux increased with increasing the mean pore size and the transmembrane pressure. The dispersed phase flux was proportional to Δp_{tm}^{x}, where exponent x was in the range of 2.3-2.7, due to a higher proportion of active pores at the higher transmembrane pressure. The minimum dispersed phase flux was 1.2-4.4 l m^{-2} h^{-1}, which was enough for 1-4 % of the pores to be active. For the same membrane (1.4 μm-α-Al_2O_3), the dispersed phase flux increased with increasing the wall shear stress, which was found earlier by Schröder [6]. It can be explained by the power function between J_d and Δp_{tm} and the larger pressure drop inside the membrane tube at the higher wall shear stress, leading to a larger variation in the local Δp_{tm} value over the membrane length.

For the SPG emulsification at $\Delta p_{tm}/p_{cap}$ = 1.1-1.5, the mean droplet size was 3.5 times larger than the mean pore size (Fig. 7), which was very similar to 3.25 found by Nakashima et al. [25] for kerosene-in-water emulsions containing SDS as an emulsifier. For MC emulsification, the mean droplet size is proportional to the equivalent diameter

of the microchannels and the proportionality constant depends on the terrace length, TL. If there are no terraces at the microchannel exits (TL = 0), $d_{3,2} = 3.0d_{eq}$ [20]. If TL is not zero, the proportionality constant is smaller, but approaches 3 as TL increases [20]. In this work $d_{3,2}/d_{eq} = 2.8$ for TL = 60 μm, which is close to 2.5-2.7 found by Kawakatsu et al. [20] for TL = 50-100 μm (Fig. 7).

Fig. 8 demonstrates that the ratio of mean droplet to mean pore size increased with increasing the $\Delta p_{tm}/p_{cap}$ ratio, both for SPG and α-Al_2O_3 membrane emulsification. However, at $\Delta p_{tm}/p_{cap} < 2$, the mean droplet size was nearly constant. For the α-Al_2O_3 membrane, a small decrease of the mean droplet size was even detected in that region. It can be explained by the assumption that when $\Delta p_{tm}/p_{cap} \rightarrow 1$, only the largest pores are active and therefore, the mean droplet size is higher than at somewhat higher pressure, when droplets are also formed at the smaller pores. Here, the smaller $d_{3,2}/d_p$ ratio was found for α-Al_2O_3 than for SPG membrane. This tendency was observed earlier by other authors [7]. Williams et al. [7] have obtained $d_{3,2}/d_p = 2.8$-2.82 for α-Al_2O_3 membranes at $d_p = 0.2$-0.5 μm, which is in good correspondence with our results at the higher $\Delta p_{tm}/p_{cap}$ values and $\sigma_w = 9$ Pa. The influence of transmembrane pressure on the mean droplet size was less significant at the higher wall shear stress. Accordingly, at the higher pressure ratios ($\Delta p_{tm}/p_{cap} > 4$), the shear stress in continuous phase must be high enough to prepare a monodispersed emulsion and to get a small mean droplet size. On the other hand, at $\Delta p_{tm}/p_{cap} < 2$, the mean droplet size is only slightly affected by the wall shear stress and therefore, it is unnecessary to apply high continuous phase flow rates under such conditions.

In the case of ME at $\Delta p_{tm}/p_{cap} < 2$, the mean droplet size was almost independent on the dispersed phase content up to 20 vol. %, as shown in Fig. 9. A small decrease of $d_{3,2}$

of 1.1-1.3 % was even observed at φ = 1.2-5 vol. %. Presumably, at the beginning of the emulsification process the smaller pores are inactive, which leads to a slightly higher mean pore size at the initial stage of the process. In the subsequent stage, the smaller pores become more and more active. The microfluidizer® (MF) is able to produce smaller droplets than membranes, but the mean droplet size is more influenced by the dispersed phase content, which can be explained by the partial droplet coalescence immediately after disruption. It is especially pronounced at the higher homogenizing pressures ($p_h \geq 70$ MPa). As an example, at p_h = 70-110 MPa the mean droplet size increased by the factor of 2.3 in the range of 1-20 vol. % (Tab. 1). On the other hand, in the same range of the dispersed phase content, the mean droplet size increased only by 11 % for the 1.4 μm-α-Al_2O_3 membrane and less than 4 % for the SPG membranes.

Fig. 10 clearly shows that the mean droplet size decreased with increasing the wall shear stress, σ_w, both for α-Al_2O_3 and SPG membranes. The influence of wall shear stress was especially large at $\sigma_w < 10$ Pa and much more significant for higher $\Delta p_{tm}/p_{cap}$ values and larger mean pore sizes. As an example, for the 4.8-μm SPG membrane $d_{3,2}/d_p$ decreased by 15 % as σ_w increased from 3.5 to 40 Pa. Over the same range of σ_w and at the similar pressure ratio, the $d_{3,2}/d_p$ ratio decreased by 8 % for the 3.1-μm SPG membrane and by less than 2 % for the 1.4-μm α-Al_2O_3 membrane. It is in accordance with the results of Schröder and Schubert [26], who found that the influence of wall shear stress on the mean droplet size was much more significant for a 0.8-μm than for 0.1-μm α-Al_2O_3 membrane. According to them, the further decrease in mean droplet size at high wall shear stresses is prevented by the rough membrane surface and the forming droplets hindering each other in detaching from the pores [26].

3.4. Influence of operating parameters on the proportion of active pores

As shown in Fig. 11, at the same $\Delta p_{tm}/p_{cap}$ ratio the proportion of simultaneously active pores was higher for the α-Al_2O_3 than for SPG membrane, due to much smaller thickness of active layer in the former case (20-40 vs. 650 μm). The proportion of simultaneously active pores was calculated using the equation given in our previous work [22].

In order to avoid contact between two rigid neighboring droplets at the pore openings, the fraction of active pores in the case of the square pore arrangement must be kept below $k_{max} = (\pi/4\varepsilon)(d_{drop}/d_p)^{-2}$ [22]. The mean porosity of the SPG membranes used in this work was 0.58 and the mean droplet/pore size ratio was typically in the range of 3-4, as shown in Figs 8 and 10. Therefore, to avoid any contact between droplets at the surface of the SPG membrane, the proportion of active pores must be kept below 8-15 %, depending on the exact droplet/pore size ratio at $k = k_{max}$. For the conditions as in Fig. 11, k_{max} for the SPG membrane was 8.5 %. If one takes into account droplet deformation in the direction of continuous phase flow, as suggested by Abrahamse et al. [27], the proportion of active pores have to be even smaller. The maximum proportion of active pores for unhindered droplet growth is substantially higher for the α-Al_2O_3 membrane (29 % for the conditions given in Fig. 11), due to the smaller porosity of active layer and the smaller d_{drop}/d_p ratio.

For both membrane type, coalescence due to steric hindrance occurred at $\Delta p_{tm}/p_{cap}$ = 5-6, which was the abscissa of the point of intersection of the curves $k = f(\Delta p_{tm}/p_{cap})$ and $k_{max} = f(\Delta p_{tm}/p_{cap})$. It is in agreement with a substantial increase of the span of droplet size distribution for the SPG membrane at $\Delta p_{tm}/p_{cap} = 5$ (Fig. 12). Therefore, in order to obtain a monodispersed emulsion, the transmembrane pressure should not be above 5-6

times larger than the capillary pressure. At the wall shear stress of 47 Pa, the span of droplet size distribution for the α-Al_2O_3 membrane was nearly constant (0.47-0.50) in the $\Delta p_{tm}/p_{cap}$ range of 1-4, but still higher than for the SPG membrane at 30 Pa. However, at the wall shear stress of 8 Pa, the span value for the emulsions prepared using the same α-Al_2O_3 membrane rapidly increased at $\Delta p_{tm}/p_{cap} > 3$. It confirms that at high pressure ratios, the wall shear stress should be relatively high for a successful operation.

4. Conclusions

The microporous membranes (SPG and ceramic α-Al_2O_3) were successfully used to produce O/W emulsions with the span of droplet size distribution of 0.26-0.59 at the transmembrane to capillary pressure ratio of less than 5-6. For the same pore size and under the same experimental conditions, the droplet size distribution was narrower in the emulsions prepared by using the SPG than α-Al_2O_3 membrane. The calculated maximum proportion of active pores for unhindered droplet growth was higher for the α-Al_2O_3 membrane, due to a smaller porosity of the active layer. The actual proportion of active pores was also higher for this membrane, due to smaller thickness of active layer. By using a silicon MC plate, the emulsion with a span value of 0.45 was produced, which was at the upper limit for the SPG membrane. For preparing O/W emulsions with the mean droplet size of less than 0.3 μm, the microfuidization is a more appropriate method than membrane emulsification. However, the span of droplet size distribution for the emulsions produced by the microfluidization was in the range of 0.9-2.7. The additional disadvantage of the microfluidizer® is that the mean droplet size is more influenced by the dispersed phase content, especially at high homogenizing

pressures.

5. List of Symbols

d_{eq} equivalent diameter of microchannels, m

d_p mean pore size of membrane, m

d_{drop} droplet diameter, m

$d_{3,2}$ mean Sauter diameter, m

J_d dispersed phase flux through membrane, m s^{-1}

J_w pure water flux through membrane, m s^{-1}

k actual proportion of active pores, (-)

k_{max} maximum proportion of active pores for unhindered droplet growth, (-)

p_{cap} cappilary pressure, Pa

p_h homogenizing pressure in the microfluidizer®, Pa

R_m hydraulic membrane resistance, m^{-1}

TL terrace length of microchannels, m

Δp_{tm} transmembrane pressure, Pa

δ_m membrane thickness, m

ε membrane porosity, (-)

η_w viscosity of water, Pa s

ξ mean tortuosity factor of pores, (-)

σ_w shear stress in continuous phase at membrane surface (wall shear stress), Pa

φ dispersed phase concentration in emulsion, vol. %

Acknowledgement.

The authors wish to thank the Alexander von Humboldt Foundation, Bonn, Germany for the financial support of this work.

References

[1] O. Behrend and H. Schubert, Ultrason. Sonochem., 8 (2001) 271-276.

[2] S.M. Joscelyne and G. Trägårdh, J. Membr. Sci., 169 (2000) 107-117.

[3] Y. Kikuchi, K. Sato, H. Ohki and T. Kaneko, Microvasc. Res., 44 (1992) 226-240.

[4] T. Nakashima and M. Shimizu, Proc. the Autumn Conference of the Society of Chemical Engineers, Japan, 1988, SB214.

[5] T. Nakashima and M. Shimizu, Ceramics Japan, 21 (1986) 408-412.

[6] V. Schröder, Ph.D. thesis, University of Karlsruhe, Germany, 1999.

[7] R.A. Williams, S.J. Peng, D.A. Wheeler, N.C. Morley, D. Taylor, M. Whalley and D.W. Houldsworth, Chem. Eng. Res. Des., 76A (1998) 902-910.

[8] S.M. Joscelyne and G. Trägårdh, J. Food Eng., 39 (1999) 59-64.

[9] M. Bendo, T. Fuchigami, H. Minakuchi, K. Nakanishi and K. Hosoya, Proceed. of the 38th SPG Forum, Miyazaki, Japan, 2002, 86-87.

[10] P.J. Dowding, J.W. Goodwin and B. Vincent, Colloid. Surface. A, 180 (2001) 301-309.

[11] G.T. Vladisavljević, S. Brösel and H. Schubert, Chem. Eng. Process., 41 (2002) 231-238.

[12] K. Suzuki, I. Fujiki and Y. Hagura, Food Sci. Technol. Int. Tokyo, 4 (1998) 164-167.

[13] I. Kobayashi, M. Yasuno, S. Iwamoto, A. Shono, K. Satoh and M. Nakajima, Colloid. Surface. A, 207 (2002) 185-196.

[14] A.J. Abrahamse, R. van Lierop, R.G.M. van der Sman, A. van der Padt and R.M. Boom, J. Membr. Sci., 204 (2002) 125-137.

[15] N. Yamazaki, H. Yuyama, M. Nagai, G.H. Ma and S. Omi, Journal of Dispersion Science and Technology, 23 (2002) 279-292.

[16] R.O. Cliff, V. Kwasiborski and A.S. Rudolph, U.S. patent No. 5,419,892, May 30, 1995.

[17] W.P. Cacheris and L. Meeh, U.S. patent No. 5,560,902, Jan. 10, 1996.

[18] A. Lemay, P. Paquin and C. Lacroix, J. Dairy Sci., 77 (1994) 2870-2879.

[19] Y.J. Shih, U.S. patent No. 5,219,924, June 15, 1993.

[20] T. Kawakatsu, Y. Kikuchi and M. Nakajima, J. Am. Oil Chem. Soc., 74 (1997) 317-321.

[21] M. Shimizu, T. Nakashima and M. Kukizaki, Kagaku Kogaku Robunshu, 28 (2002) 310-316.

[22] G.T. Vladisavljević and H. Schubert, Desalination, 144 (2002) 167-172.

[23] T. Nakashima and M. Shimizu, Kagaku Kogaku Ronbunshu, 19 (1993) 984-990.

[24] M. Shimizu, personal communication, 2002.

[25] T. Nakashima, M. Shimizu and M. Kukizaki, Adv. Drug. Deliv. Rev., 45 (2000) 47-56.

[26] V. Schröder and H. Schubert, Colloid. Surface. A, 152 (1999) 103-109.

[27] A.J. Abrahamse, A. van der Padt, R.M. Boom and W.B.C. de Heij, AIChE J., 47 (2001) 1285-1291.

TABLES

Table 1. Mean droplet size and the span of the droplet size distribution as a function of the homogenizing pressure and dispersed phase content for the emulsions prepared by the microfluidization.

P_h (MPa)	1 vol. %		2.5 vol. %		5 vol. %		10 vol. %		20 vol. %		30 vol. %		40 vol. %		50 vol. %	
	$d_{3,2}$ (μm)	span	$d_{3,2}$ (μm)	span	$d_{3,2}$ (μm)	Span	$d_{3,2}$ (μm)	span	$d_{3,2}$ (μm)	span	$d_{3,2}$ (μm)	span	$d_{3,2}$ (μm)	span	$d_{3,2}$ (μm)	span
5	0.71	2.3	0.71	2.3	0.78	2.2	0.85	2.1	0.97	2.1	1.2	1.9	1.3	1.6	2.1	1.2
10	0.54	2.7	0.56	2.7	0.62	2.6	0.67	2.3	0.80	2.2	0.95	1.8	1.1	1.5	1.6	1.1
20	0.35	2.6	0.40	2.6	0.49	2.3	0.50	2.5	0.72	2.0	0.76	1.4	0.95	1.3	1.4	1.1
30	0.24	2.5	0.30	2.1	0.32	2.2	0.44	2.2	0.52	1.9	0.71	1.2	0.85	1.1	1.1	1.1
50	0.20	2.1	0.22	1.8	0.21	1.7	0.36	1.6	0.47	1.4	0.55	1.4	0.76	1.1	-	-
70	0.17	2.1	0.18	1.9	0.20	1.6	0.29	1.2	0.39	0.97	0.55	1.3	0.76	0.99	1.0	1.0
110	0.16	2.1	0.15	2.2	0.16	2.1	0.25	1.3	0.37	0.92	0.66	0.91	0.69	0.95	-	-
2×110	0.087	1.1	0.085	0.94	0.093	1.1	0.10	1.2	0.30	1.0	0.49	1.2	-	-	1.0	1.0

FIGURE CAPTIONS

Figure 1. Schematic diagram of the cross-flow membrane emulsification system used in this study (−··−·· compressed air line, ····· dispersed phase line, ——— continuous phase or emulsion line, - - - - - - cleaning line).

Figure 2. Schematic diagram of the experimental system used for microfluidization.

Figure 3. Plot of transmembrane flux vs. pressure for the permeation of pure water through the SPG and α-Al_2O_3 membranes of different pore sizes (batch = small SPG tube with an effective membrane area of 4 cm^2).

Figure 4. Hydraulic resistance of the the SPG and α-Al_2O_3 membranes used in this work.

Figure 5. Influence of emulsification method on droplet size distribution (dispersed phase content $\varphi \approx 1$ vol. %).

Figure 6. The influence of transmembrane pressure on the dispersed phase flux for the SPG and α-Al_2O_3 membranes.

Figure 7. Mean droplet size as a function of the mean pore size (for SPG and α-Al_2O_3 membranes) or the equivalent diameter of the microchannels (for MC emulsification, TL = terrace length).

Figure 8. The variation of mean droplet/pore size ratio with the pressure ratio.

Figure 9. The influence of dispersed phase concentration on the mean droplet size for different emulsification methods (ME = membrane emulsification at Δp_{tm} = 1.1-2.2p_{cap}, MF = microfluidization at different homogenizing pressures).

Figure 10. The variation of mean droplet size with the wall shear stress (dispersed phase content $\varphi \approx 1$ vol. %).

Figure 11. Maximum and actual proportion of active pores vs. pressure ratio for the SPG and α-Al_2O_3 membranes.

Figure 12. The influence of pressure ratio on the span of the droplet size distribution for the SPG and α-Al_2O_3 membrane (operating conditions as in Fig 11).

FIGURES

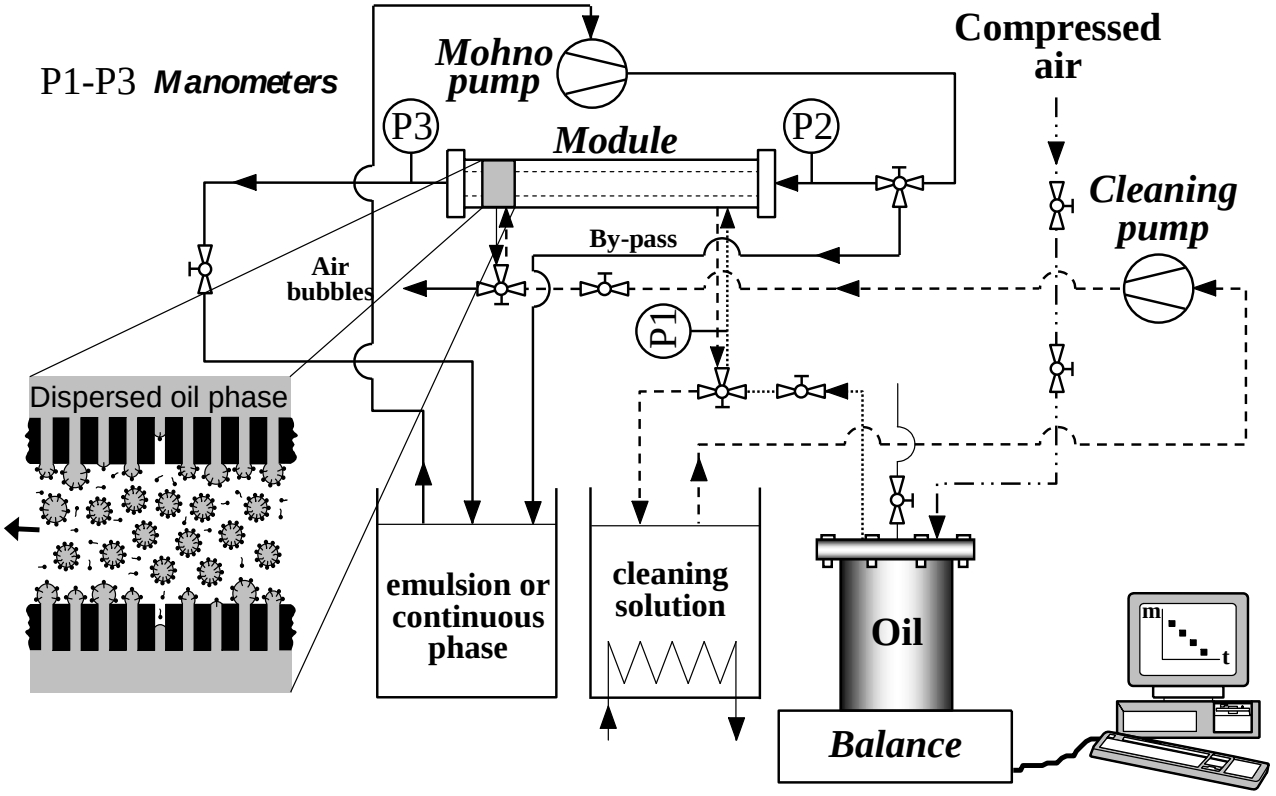

Fig. 1

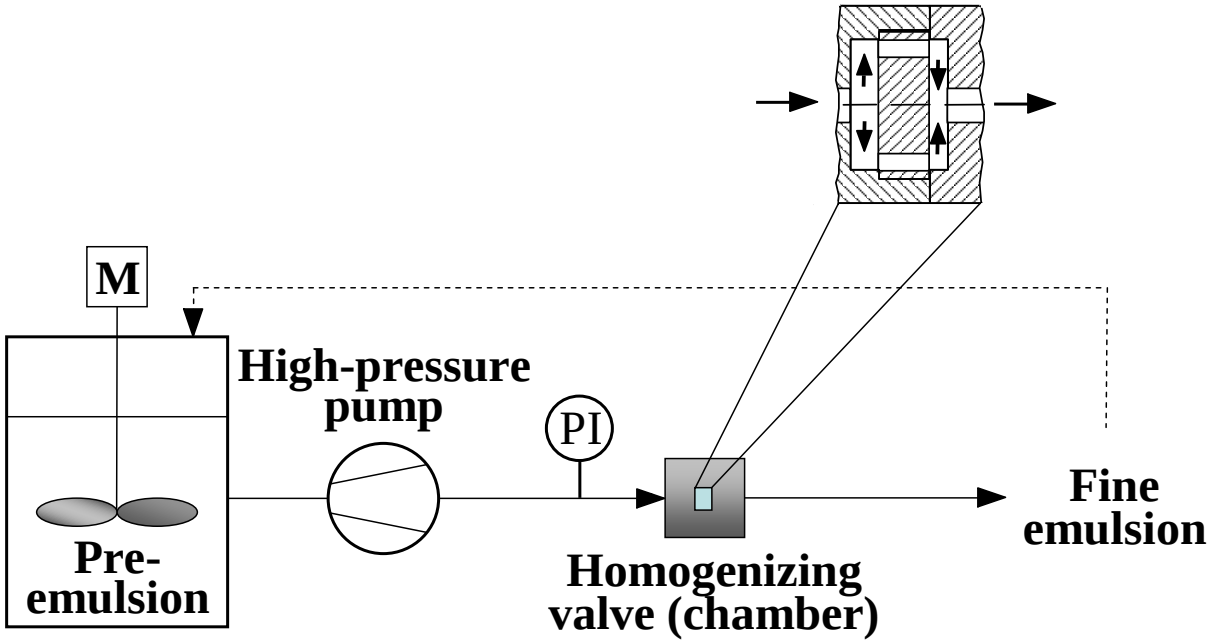
M
High-pressure
pump
PI
Pre-
emulsion
Homogenizing
valve (chamber)
Fine
emulsion

Fig. 2

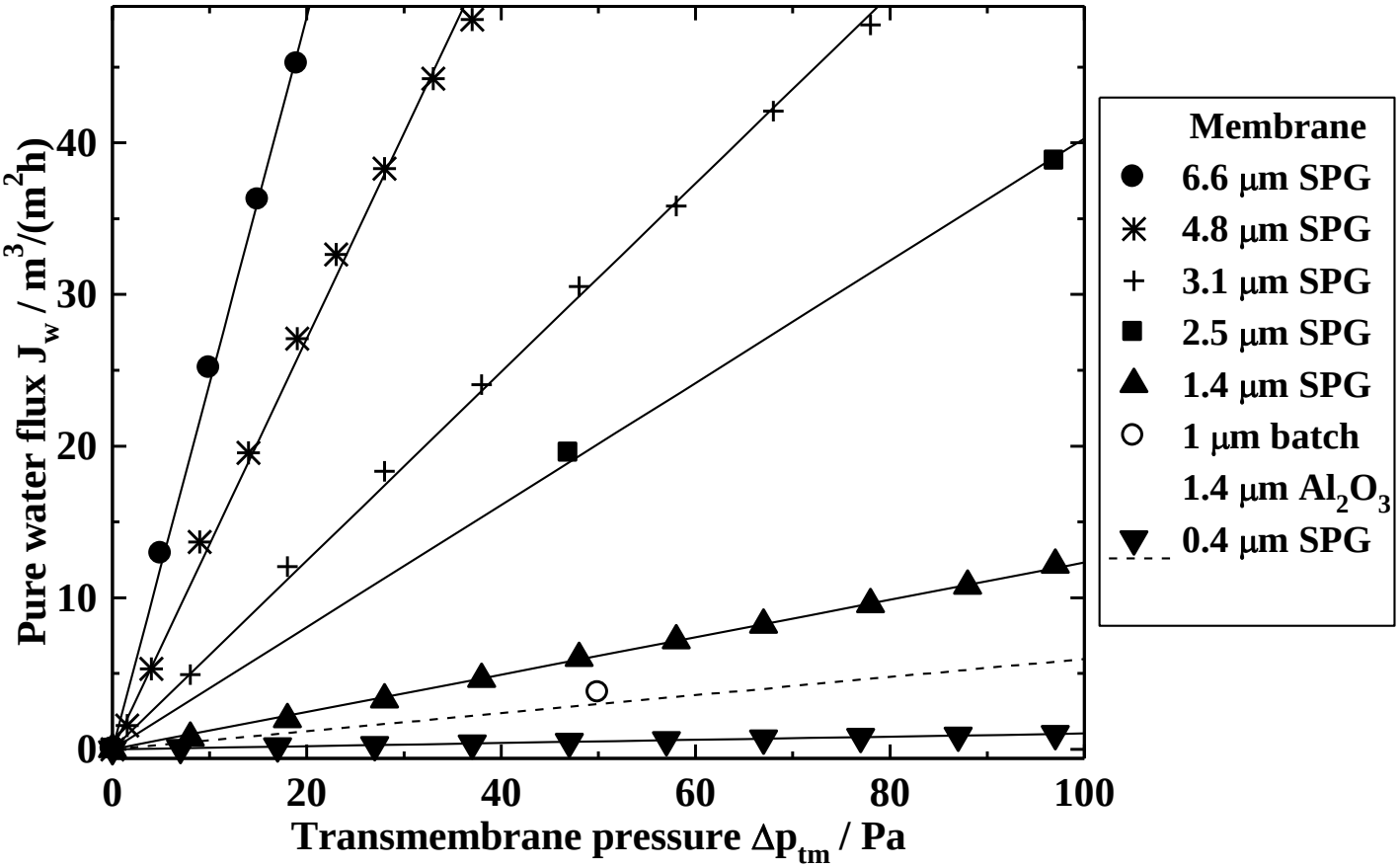
Pure water flux J_w / $m^3/(m^2h)$
Transmembrane pressure Δp_{tm} / Pa
0
10
20
30
40
0
20
40
60
80
100
Membrane
6.6 μm SPG
4.8 μm SPG
3.1 μm SPG
2.5 μm SPG
1.4 μm SPG
1 μm batch
1.4 μm Al_2O_3
0.4 μm SPG

Fig. 3

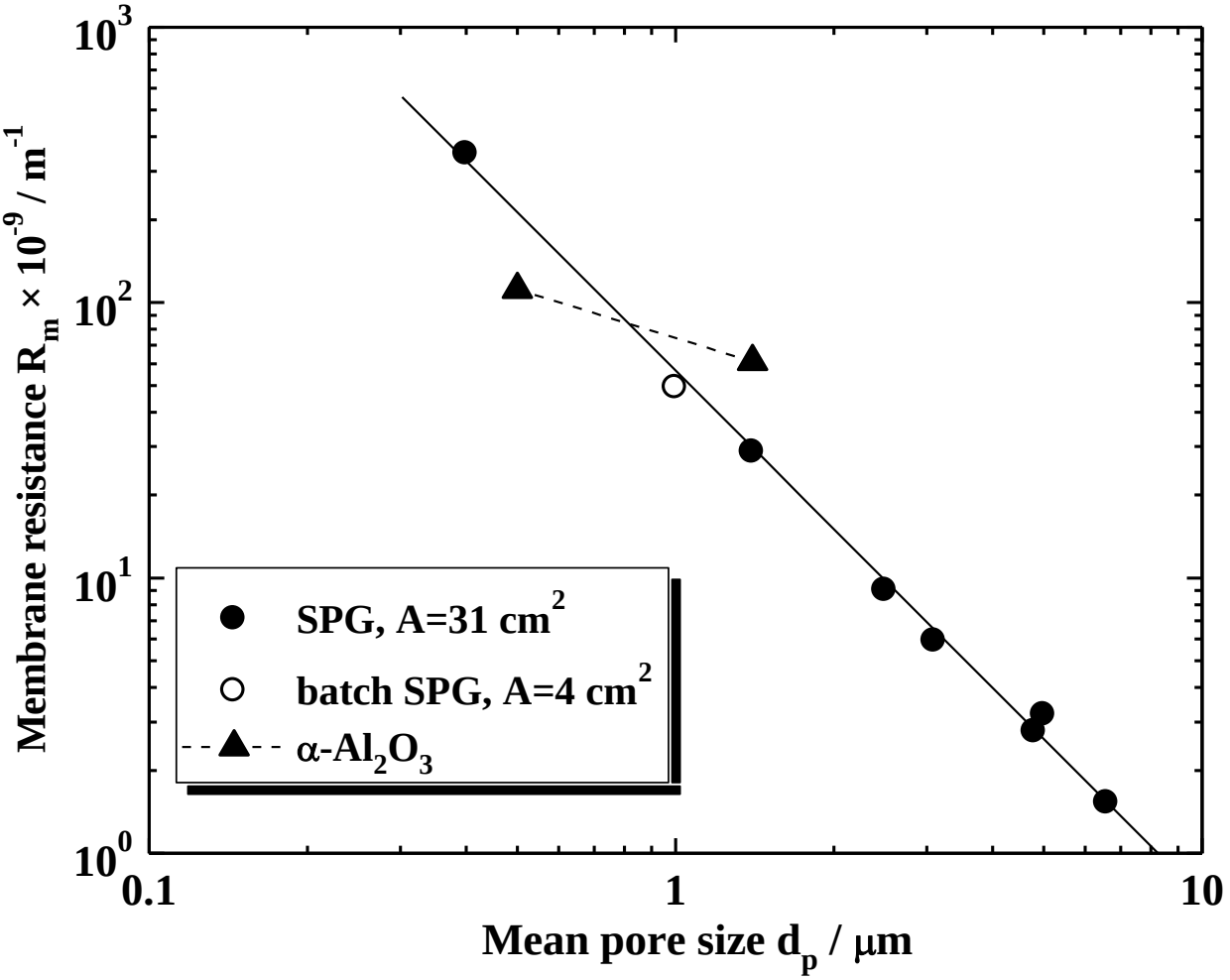
Membrane resistance $R_m \times 10^{-9}$ / m^{-1}
10^3
10^2
10^1
10^0
0.1
1
10
Mean pore size d_p / μm
SPG, A=31 cm^2
batch SPG, A=4 cm^2
α-Al_2O_3

Fig. 4

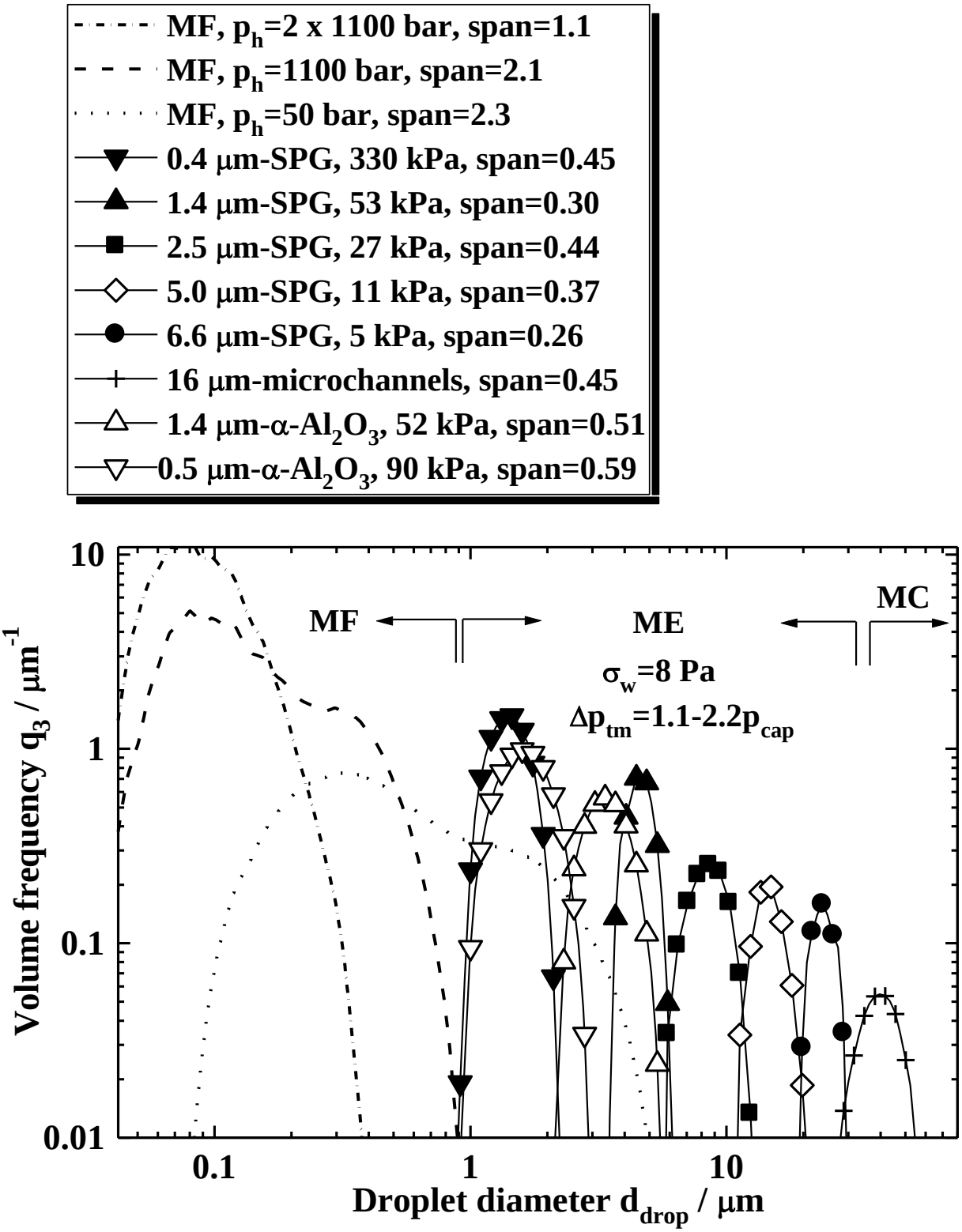
MF, p_h=2 x 1100 bar, span=1.1
MF, p_h=1100 bar, span=2.1
MF, p_h=50 bar, span=2.3
0.4 μm-SPG, 330 kPa, span=0.45
1.4 μm-SPG, 53 kPa, span=0.30
2.5 μm-SPG, 27 kPa, span=0.44
5.0 μm-SPG, 11 kPa, span=0.37
6.6 μm-SPG, 5 kPa, span=0.26
16 μm-microchannels, span=0.45
1.4 μm-α-Al2O3, 52 kPa, span=0.51
0.5 μm-α-Al2O3, 90 kPa, span=0.59
MF
ME
MC
σw=8 Pa
Δptm=1.1-2.2pcap
Volume frequency q3 / μm-1
Droplet diameter ddrop / μm
10
1
0.1
0.01
0.1
1
10

Fig. 5

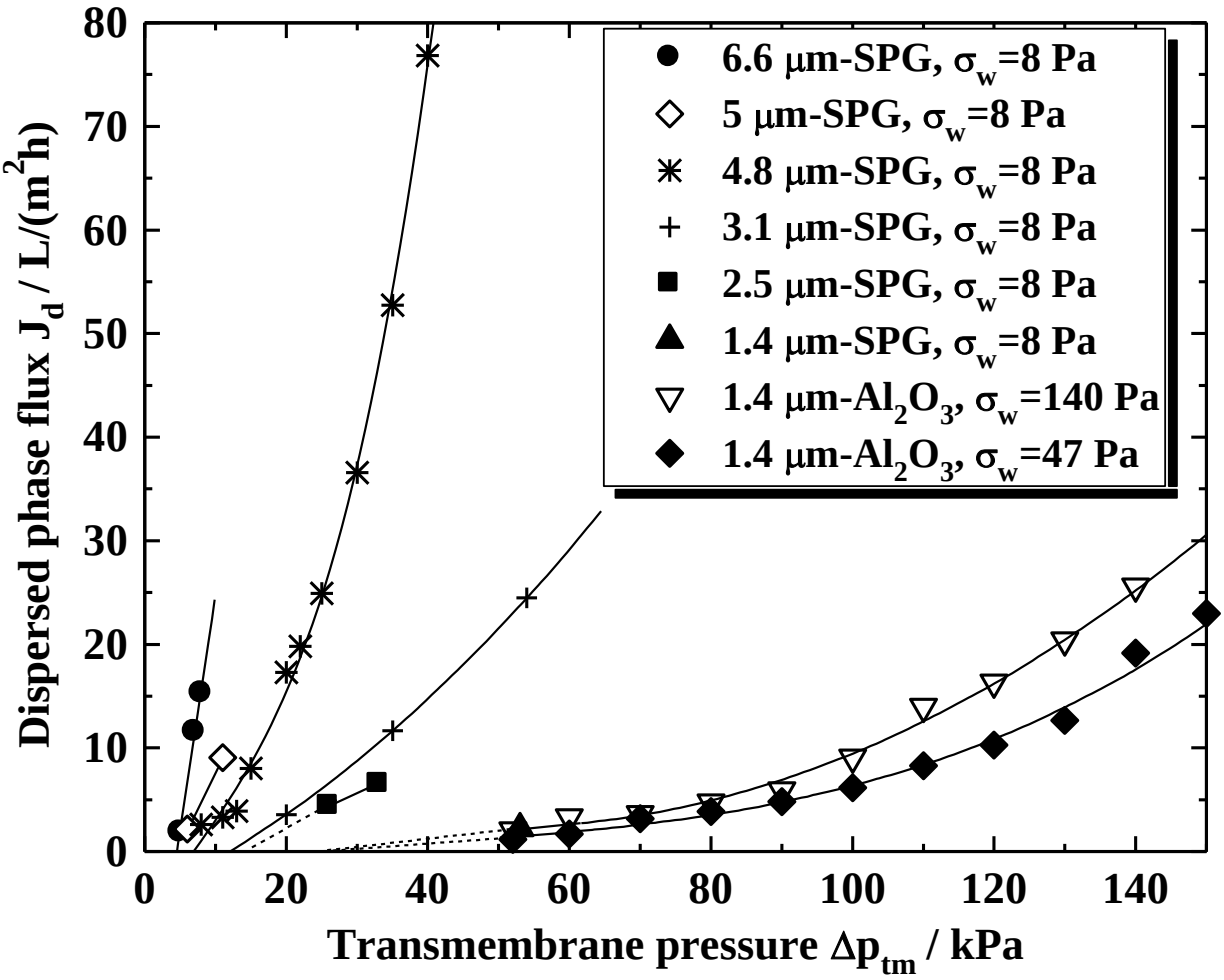
Dispersed phase flux J_d / L/(m^{2}h)
Transmembrane pressure Δp_{tm} / kPa
0
10
20
30
40
50
60
70
80
0
20
40
60
80
100
120
140
6.6 μm-SPG, σ_w=8 Pa
5 μm-SPG, σ_w=8 Pa
4.8 μm-SPG, σ_w=8 Pa
3.1 μm-SPG, σ_w=8 Pa
2.5 μm-SPG, σ_w=8 Pa
1.4 μm-SPG, σ_w=8 Pa
1.4 μm-Al_2O_3, σ_w=140 Pa
1.4 μm-Al_2O_3, σ_w=47 Pa

Fig. 6

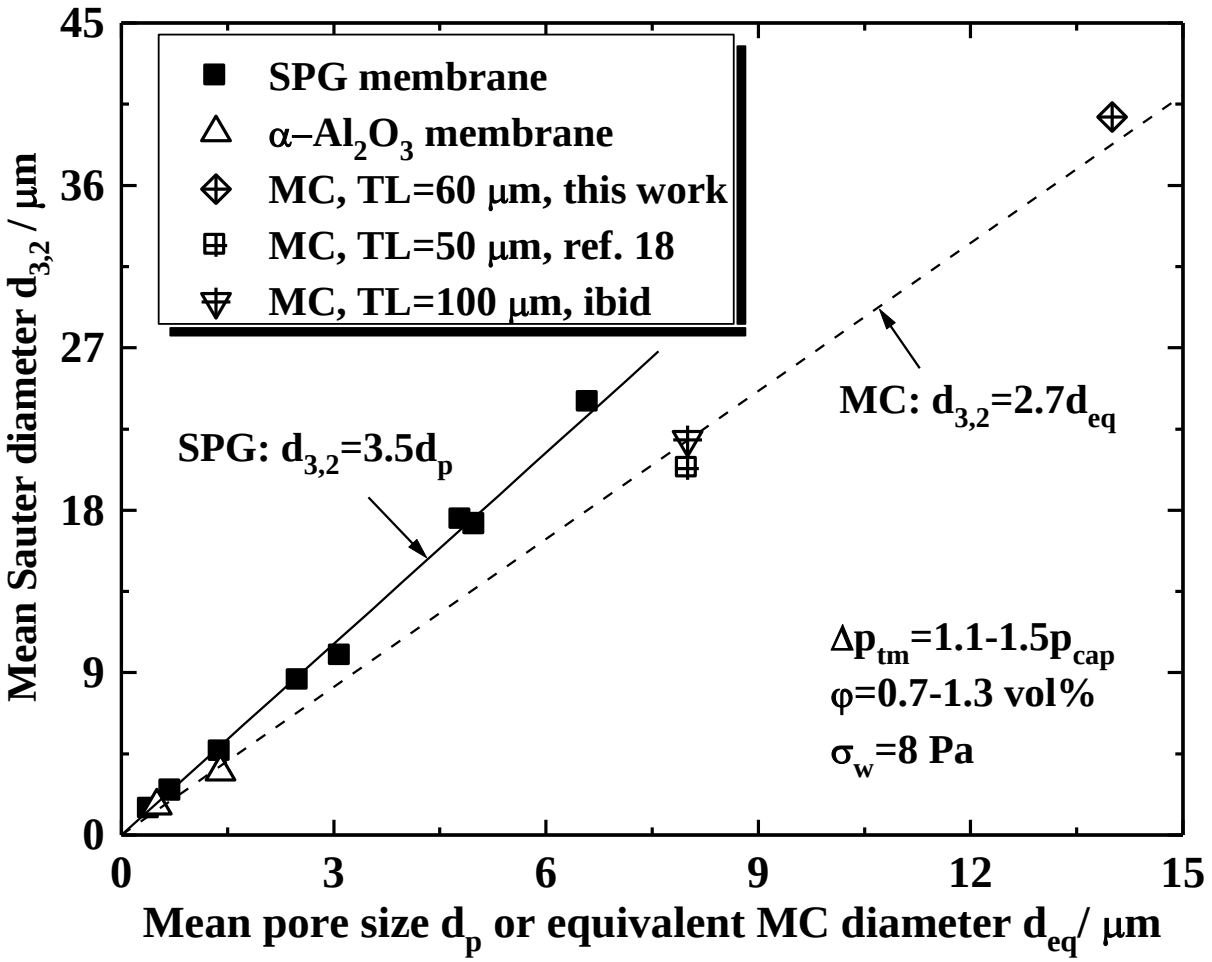
SPG membrane
α–Al2O3 membrane
MC, TL=60 μm, this work
MC, TL=50 μm, ref. 18
MC, TL=100 μm, ibid
SPG: d3,2=3.5dp
MC: d3,2=2.7deq
Δptm=1.1-1.5pcap
φ=0.7-1.3 vol%
σw=8 Pa
Mean Sauter diameter d3,2 / μm
Mean pore size dp or equivalent MC diameter deq/ μm
0
9
18
27
36
45
0
3
6
9
12
15

Fig. 7

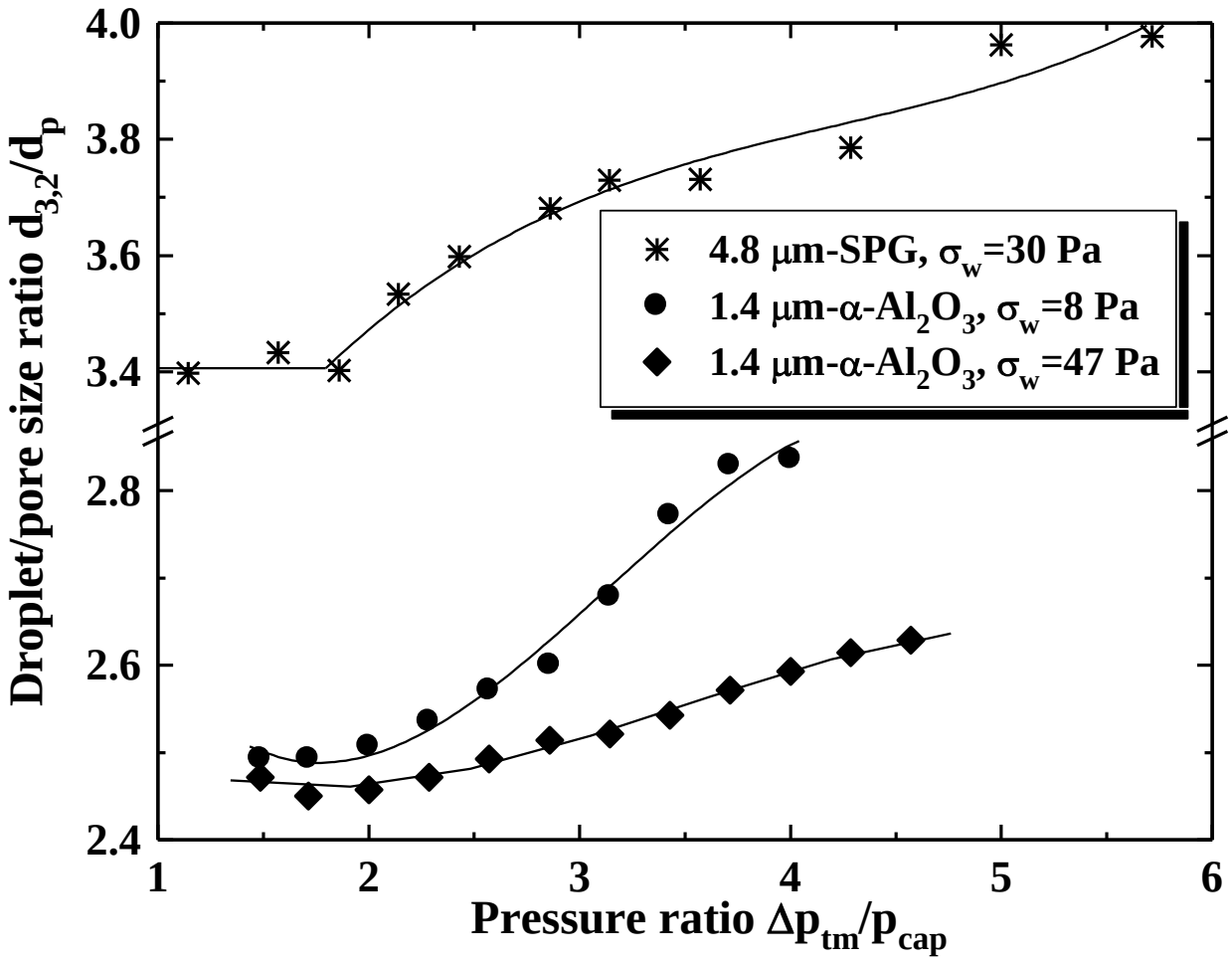
4.0
3.8
3.6
3.4
2.8
2.6
2.4
1
2
3
4
5
6
Droplet/pore size ratio $d_{3,2}/d_p$
Pressure ratio $\Delta p_{tm}/p_{cap}$
4.8 μm-SPG, σ_w=30 Pa
1.4 μm-α-Al_2O_3, σ_w=8 Pa
1.4 μm-α-Al_2O_3, σ_w=47 Pa

Fig. 8

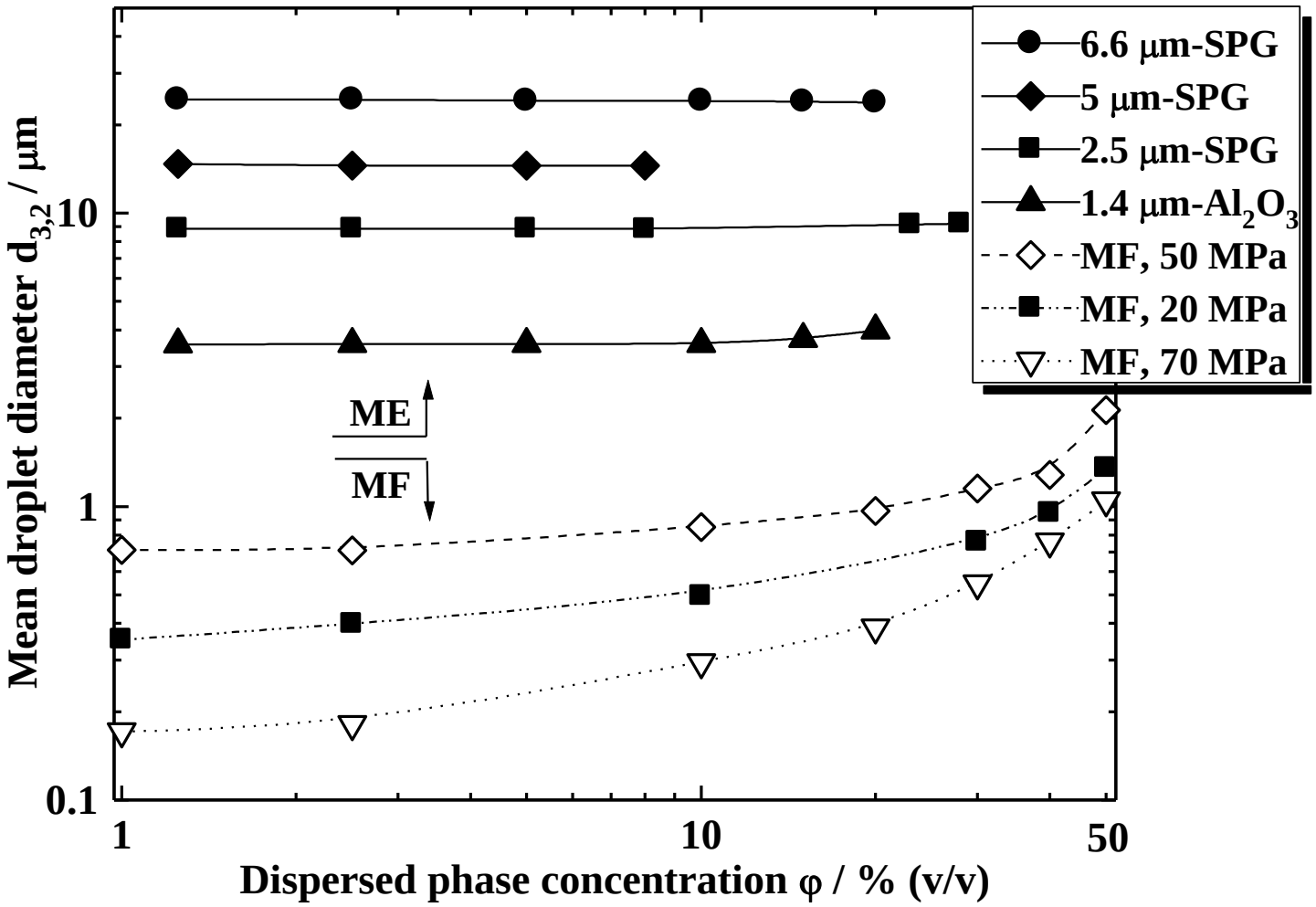
6.6 μm-SPG
5 μm-SPG
2.5 μm-SPG
1.4 μm-Al2O3
MF, 50 MPa
MF, 20 MPa
MF, 70 MPa
ME
MF
Mean droplet diameter d3,2 / μm
10
1
0.1
1
10
50
Dispersed phase concentration φ / % (v/v)

Fig. 9

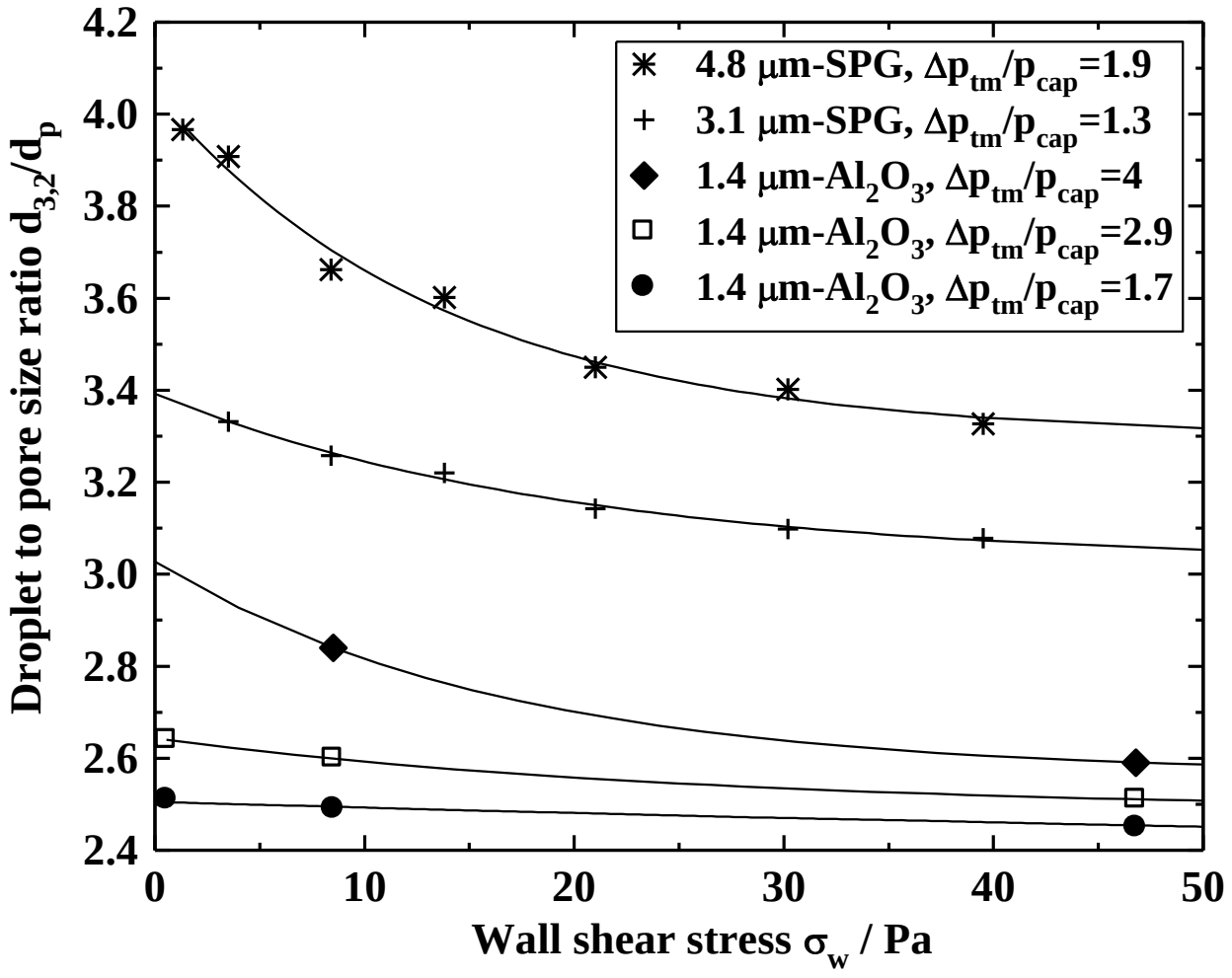
4.8 μm-SPG, Δp_tm/p_cap=1.9
3.1 μm-SPG, Δp_tm/p_cap=1.3
1.4 μm-Al2O3, Δp_tm/p_cap=4
1.4 μm-Al2O3, Δp_tm/p_cap=2.9
1.4 μm-Al2O3, Δp_tm/p_cap=1.7
Droplet to pore size ratio d3,2/dp
Wall shear stress σw / Pa
4.2
4.0
3.8
3.6
3.4
3.2
3.0
2.8
2.6
2.4
0
10
20
30
40
50

Fig. 10

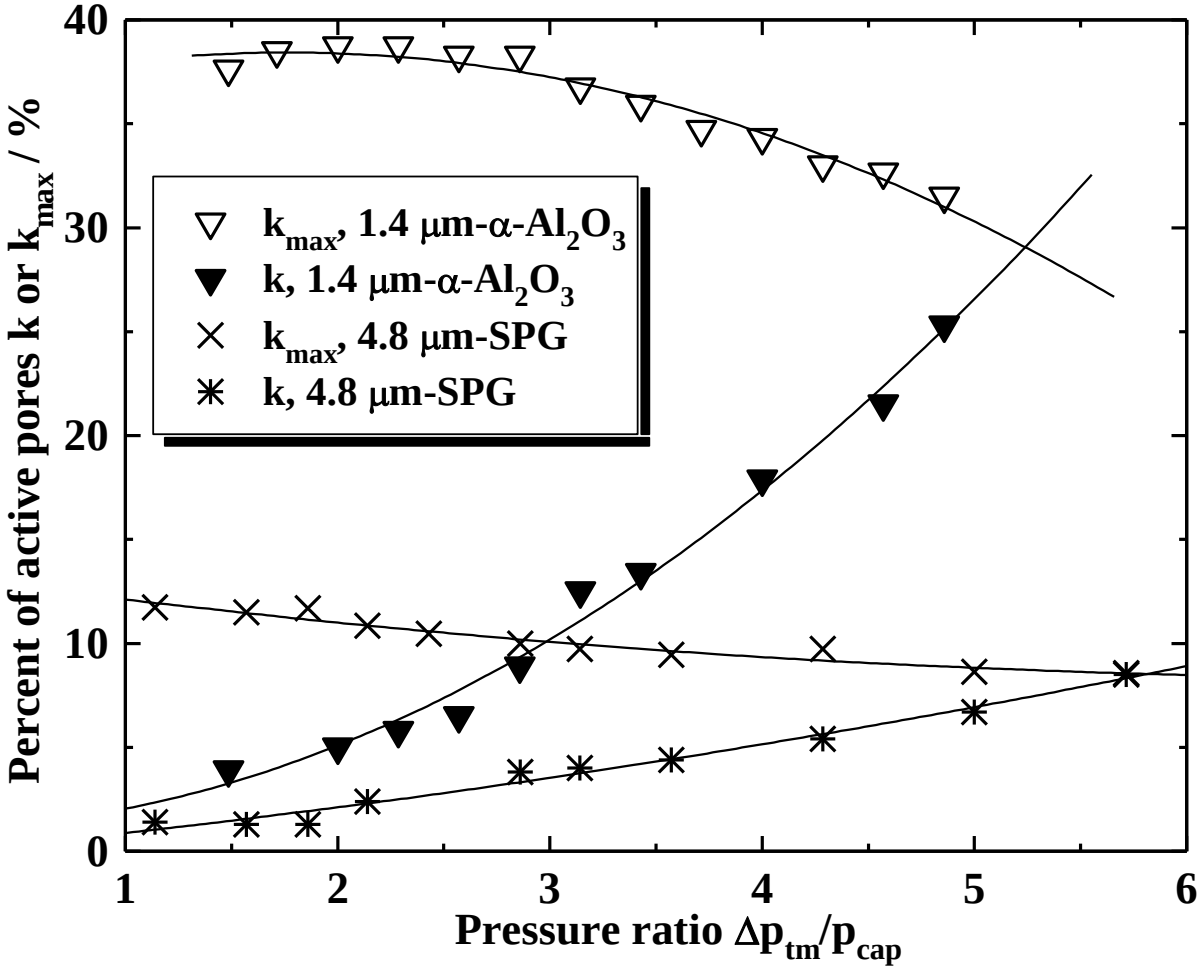
Percent of active pores k or k_{max} / %
Pressure ratio $\Delta p_{tm}/p_{cap}$
k_{max}, 1.4 μm-α-Al_2O_3
k, 1.4 μm-α-Al_2O_3
k_{max}, 4.8 μm-SPG
k, 4.8 μm-SPG
0
10
20
30
40
1
2
3
4
5
6

Fig. 11

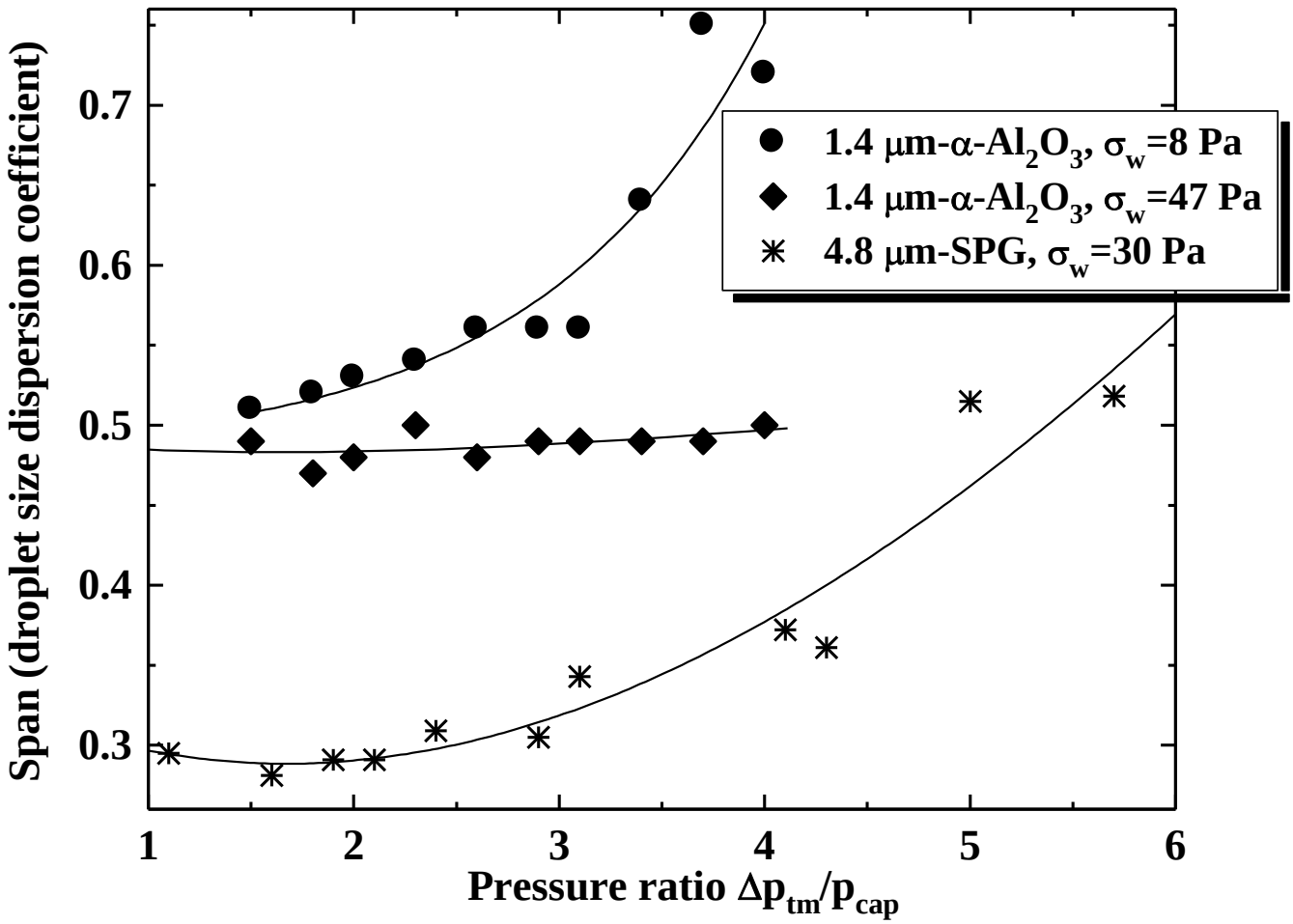
Span (droplet size dispersion coefficient)
0.3
0.4
0.5
0.6
0.7
1
2
3
4
5
6
Pressure ratio $\Delta p_{tm}/p_{cap}$
1.4 μm-α-Al_2O_3, σ_w=8 Pa
1.4 μm-α-Al_2O_3, σ_w=47 Pa
4.8 μm-SPG, σ_w=30 Pa

Fig. 12